

# A polynomial based model of input and feedback capacitances suitable for Volterra analysis

Nagaditya Poluri<sup>1</sup>, Alex Moores<sup>1</sup>, Robin Sloan<sup>2</sup>, Maria Merlyne De Souza<sup>1</sup>

1. EEE Department, University of Sheffield, Sheffield S13JD.
2. Mwave-inspect.

Contact: m.desouza@sheffield.ac.uk

In Volterra analysis, non-linearities are typically modelled using a polynomial to decompose the overall distortion at the output of an amplifier into second, third, and higher order effects that enables the contributions from capacitances and the current generator to be quantified. In this work, we explore a polynomial-based model of  $C_{gs}$  and  $C_{gd}$  that is suitable for Volterra analysis. The proposed approach resolves the problem of divergence of the polynomial beyond the range of values for which the fitting is performed. The accuracy of the proposed model is compared to that of the “tanh” function for a Ka band GaAs pHEMT. The error between the modelled and measured  $C_{gs}$  is  $< 6\%$  for the proposed model whereas the “tanh” function based model results in error of  $20\%$ .

## I. INTRODUCTION

The design of highly efficient and linear amplifiers depends upon the availability of accurate yet efficient large signal models of their underlying transistors. Amplifiers have to meet stringent linearity specifications such as  $-40$  dBc adjacent channel power ratio (ACPR) for 5G applications. Quantifying distortion originating from disparate sources such as the non-linear current generator, capacitances, impedances at the baseband, fundamental as well as harmonic frequencies, enables the designer with choices to minimize distortion [1]. In this paper, we focus on the non-linear input and feedback capacitances. The variation of the intrinsic capacitances with gate and drain bias results in distortion. In particular, the distortion of the signal due to the input capacitance contributes to intermodulation distortion, often of comparable magnitude to distortion from the current generator.

Volterra analysis has been shown to aid the selection of impedances and the bias point for high linearity [1]. In Volterra analysis, non-linearities are typically modelled using a polynomial to decompose the overall distortion at the output of the amplifier into second, third, and higher order effects from its various sources. Analytical based approaches proposed for Volterra analysis assume several approximations to derive these expressions and are cumbersome to scale with the number of parasitic elements. Alternatively, in Volterra over Harmonic Balance (VoHB) [1] [2] [3], first HB simulations are performed on an equivalent circuit model of the transistor. Currents and voltages across its components are fitted to a polynomial for each component. However, this method of polynomial fitting requires approximations, limiting the number of frequency points for analysis, to minimise complexity of the analytical expressions. Additionally, we have observed that this approach results in inaccurate results and fails to converge when the number of frequency points is increased.

In this work, we propose an accurate model of non-linear intrinsic capacitances using polynomials. Such a model enables first, second, and higher components of the distortion directly from simulation to enable a judicious choice of cancellation mechanisms. This minimizes the need of approximate analytical expressions that are prone to convergence issues

in VoHB. The proposed approach resolves the problem of divergence beyond the range of values for which fitting is performed and is more accurate when compared to the tanh function model [4], often used in literature.

## II. Background

There are two ways of modelling the Gate-to-Source capacitance,  $C_{gs}$  and the Gate-to-Drain capacitance,  $C_{gd}$ : (i) division by charge and (ii) division by capacitance [5]. Charge at the gate terminal ( $Q_g$ ) is a sum of charge from the source ( $Q_{gs}$ ) and drain ( $Q_{gd}$ ) terminals:

$$Q_g = Q_{gs} + Q_{gd} \quad (1)$$

The reactive gate current ( $I_g$ ) is given as

$$I_g = I_s + I_d \quad (2)$$

$$I_s = C_{gs} \frac{dV_{gsi}}{dt} + \frac{\partial Q_{gs}}{\partial V_{gdi}} \frac{dV_{gdi}}{dt} \quad (3)$$

$$I_d = \frac{\partial Q_{gd}}{\partial V_{gsi}} \frac{dV_{gsi}}{dt} + C_{gd} \frac{dV_{gdi}}{dt} \quad (4)$$

Where,  $\frac{\partial Q_{gd}}{\partial V_{gsi}}$  and  $\frac{\partial Q_{gs}}{\partial V_{gdi}}$  denote trans-capacitances which are difficult to determine [5].

Additionally, this approach can result in non-conservation of charge when a periodic excitation that conserves  $Q_g$  results in a non-periodic  $Q_{gs}$  and  $Q_{gd}$  [5]. Hence, division by capacitance is often used, in which case  $I_s$  and  $I_d$  are written as

$$I_s = \frac{\partial Q_{gs}}{\partial t} = \frac{\partial Q_{gs}}{\partial V_{gsi}} \frac{\partial V_{gsi}}{\partial t} = C_{gs} \frac{dV_{gsi}}{dt} \quad (5)$$

$$I_d = \frac{\partial Q_{gd}}{\partial t} = \frac{\partial Q_{gd}}{\partial V_{gdi}} \frac{\partial V_{gdi}}{\partial t} = C_{gd} \frac{dV_{gdi}}{dt} \quad (6)$$

The advantage of this representation is consistency with the small signal model of the transistor and an absence of trans-capacitance. However, a straight forward implementation of  $C_{gs} \frac{dV_{gsi}}{dt}$  results in a DC current which is unphysical [6]. Hence,  $C_{gs}$  is implemented as  $\frac{\partial Q_{gs}}{\partial V_{gsi}}$ . Nevertheless, it is still difficult to implement a differential with only one variable in HB simulations, so  $C_{gs}$  is represented as:

$$C_{gs} = \frac{\partial Q_{gs}}{\partial V_{gsi}} = \frac{Q_{gs}(V_{gsi} + dV_{gsi}, V_{dsi}) - Q_{gs}(V_{gsi}, V_{dsi})}{dV_{gsi}}$$

In an empirical approach, extracted capacitances are fitted to predetermined functions of the gate and drain voltages under the constraint that each function must be differentiable [5]. We illustrate this example using  $C_{gs}$ , modelled as a product of functions  $f$  and  $g$  of the gate and drain voltages as

$$C_{gs} \propto f(V_{gs})g(V_{ds}) \quad (7)$$

In this case, charge is calculated by integrating with terminal voltage as given in (9) and it can be implemented as in (10).

$$Q_{gs} = g(V_{ds}) \int f(V_{gs}) dV_{gs} = g(V_{ds}) Q_{pgs}(V_{gs}) \quad (8)$$

$$I_s = g(V_{ds}) \frac{dQ_{pgs}(V_{gs})}{dt} \quad (9)$$

$\frac{dQ_{pgs}(V_{gs})}{dt}$  in (10) can be implemented in ADS as  $j2\pi f Q_{pgs}(V_{gs})$ , where  $f$  is the frequency.

Simulations using HB of this model show the sum of the non-linear response in the spectral tones. However, the drawback is that the components of the spectrum originating from the first, second, and higher order non-linearities are not distinguishable [7]. For example, it is seen that IM3 is generated due to the mixing of the baseband and second harmonic content, as illustrated in Fig. 1 (a), due to the second and third order non-linearity of the transistor [1][8][9]. Volterra analysis on the other hand can distinguish the response of each distortion mechanism separately, as shown in Fig. 1 (b). These insights into the device operation and mixing mechanisms enable optimization of the design for reducing distortion. A PA designer does not have control over the non-linearities of the device but can control the conversion of distortion current generated from the non-linearities to node voltages by an appropriate choice of impedances at the baseband, fundamental and harmonic impedances presented to the device and the bias point [7].

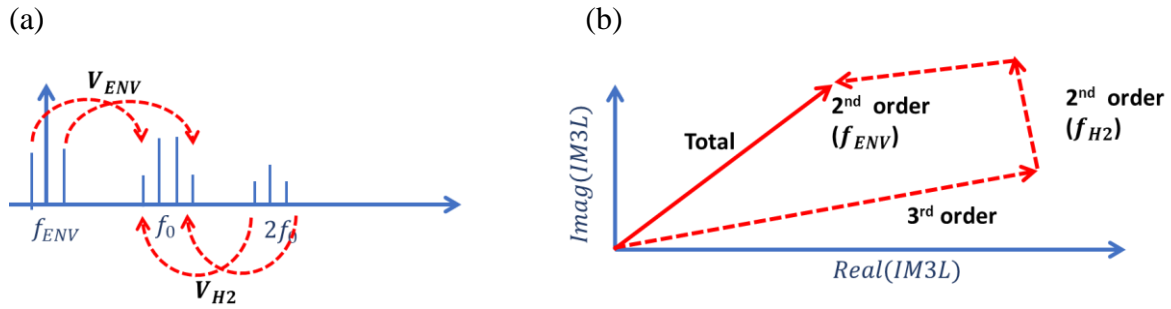


Fig. 1 (a) Output spectrum of a PA (b) Illustration of contribution of several component to the IMD3.

In Volterra analysis,  $C_{gs}$  is modelled as a polynomial as [7]:

$$C_{gs} = C_{gs00} + C_{gs10}v_{gs} + C_{gs01}v_{ds} + C_{gs11}v_{gs}v_{ds} + \dots \quad (10)$$

Numerical techniques can be used to calculate the coefficients ( $C_{gs00}$ ,  $C_{gs01}$ ,  $C_{gs10}$ , ...) whose derivatives are devoid of discontinuities. However, polynomial functions are accurate for a limited range of data. For example, measured  $C_{gs}$  outside the range of data used to generate the

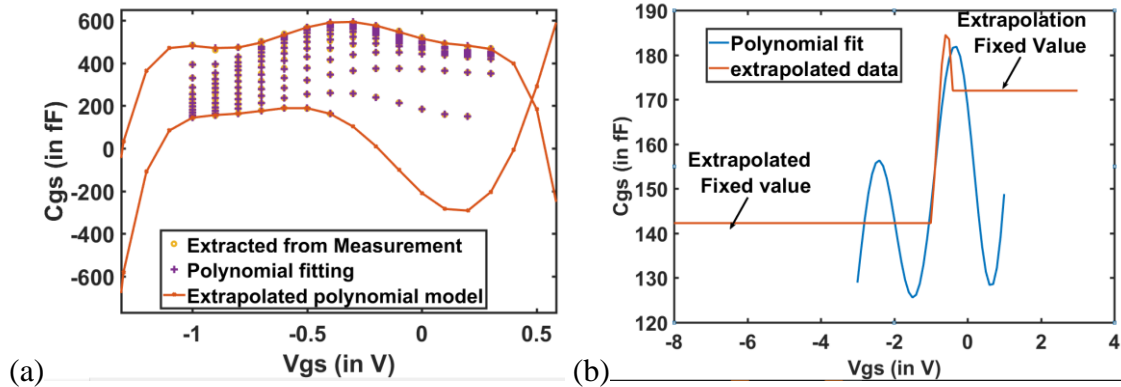


Fig 2(a) Plot of Measured data and extrapolated polynomial fit. (b) Polynomial fit with extrapolated data.

polynomial can result in undesirable behaviour, as shown in Fig. 2 (a). Additionally, a small variation in the measured data due to noise may result in large changes in the polynomial coefficients leading to un-realistic derivatives.

### III. Proposed polynomial model for the intrinsic $C_{gs}$ and $C_{gd}$

In our approach, we express capacitances as

$$C_{gs}(V_{gs}, V_{ds}) = \sum_{n=0}^N f_{gs(n)}(V_{gs}) g_{(n)}(V_{ds}) \quad (11)$$

$$C_{gd}(V_{gs}, V_{gd}) = \sum_{n=0}^N g_{gd(n)}(V_{gs}) g_{(n)}(V_{gs} - V_{gd}) \quad (12)$$

We implement these as:

$$g_{(n)}(V_{ds}) = \begin{cases} (1 - V_{ds}/V_{dsq})^n & 0 < V_{ds} < V_{dsq} \\ 0 & V_{ds} > V_{dsq} \end{cases} \quad (13)$$

It is seen that  $g_{(n)}(V_{ds})$  denotes the  $n$ th power of the RF component of the  $V_{ds}$ .  $f_{gs(n)}(V_{gs})$  and  $g_{gd(n)}(V_{gs})$  are obtained from the curve fitting tool in matlab and read as a table in ADS. For all values of  $n > 1$ , this function is continuous at  $V_{ds} = V_M$ . However, the first order derivative for  $n=1$  is 1 at  $V_{ds} = V_M$  resulting in a discontinuous derivative. The definition of  $g_{(n)}(V_{ds})$  ensures that the model does not diverge beyond measurement range for  $V_{ds} > 0$ . The model diverges for  $V_{ds} < 0$  which is never required. Hence, we use a cubic spline to fit this case after the determination of  $f_{gs(n)}(V_{gs})$ . In equation (14),  $V_M$  is either the value of  $V_{ds}$  up to which measurement is performed or the  $V_{ds}$  beyond which  $C_{gs}$  and  $C_{gd}$  have a minimum dependence on  $V_{ds}$ . The proposed capacitor model is implemented as a power series of the drain voltage, where each term in (12) and (13) i.e.,  $g_{gd(n)}(V_{gs})x^n$  and  $f_{gs(n)}(V_{gs})x^n$  denote the contribution to the distortion due to the  $n$ th order non-linear dependence of the capacitor on the drain voltage, simplifying the VoHB analysis.

### IV. Model application

To demonstrate the proposed model, we have extracted and modelled non-linear  $C_{gs}$  and  $C_{gd}$  from measured multi bias S-parameters of a  $4 \times 75 \text{ um}$  100-nm GaAs pHEMT device. The gate and drain bias is swept from the subthreshold to linear to saturation regions. We have used the extraction procedure outlined in [10][11] to extract the parasitic  $C_{gs}$  and  $C_{gd}$  followed by optimization to achieve an error less than 5% between the modelled and predicted s-parameters over the frequency range 0.1-40 GHz. The extracted values are fitted to the polynomial models proposed in (12) and (13) for several values of  $N$ . The error between the measured and modelled  $C_{gs}$  as  $N$  is increased from 1 to 5 is plotted in Fig. 3. An error  $< 7\%$  is observed even for  $N=1$ . We observe that there is no significant reduction in error for  $N > 2$ . Hence we choose  $N=2$  for the implementation of  $C_{gs}$ .

Following a similar procedure for  $C_{gd}$ , the results for  $C_{gs}$  plotted in Fig. 3 give a choice of  $N=4$  with no further improvement for  $N=5$ . The extracted values of  $C_{gs}$  and  $C_{gd}$  are compared with the proposed polynomial model for  $N=2$  and  $N=4$  respectively in Fig. 4. A close match between the model and measurement is observed.

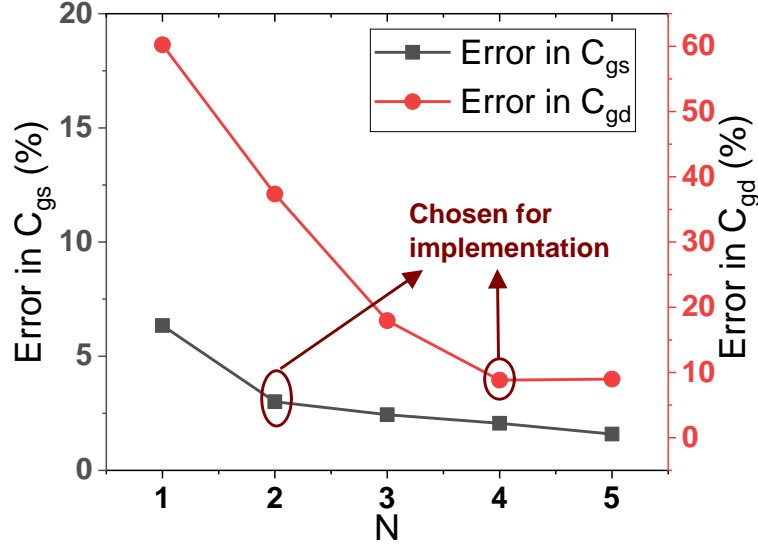


Fig. 3. Error between the measured and modelled  $C_{gs}$  and  $C_{gd}$  versus the order of N.

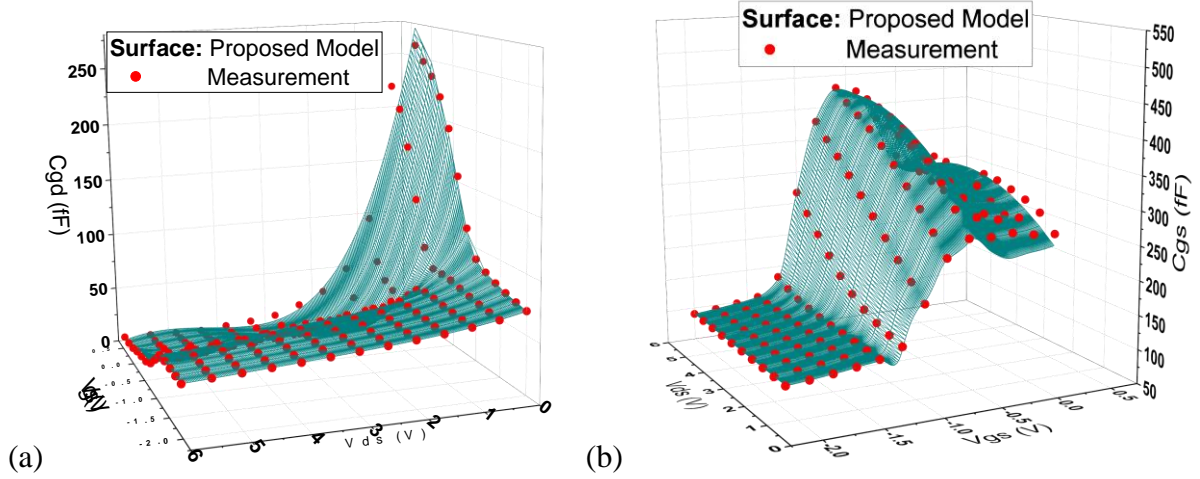


Fig. 4. The extracted values compared with the proposed polynomial model (a)  $C_{gd}$  (N=2) and (b)  $C_{gs}$  (N=4).

In Fig 5, the  $C_{gs}$  is modelled using tanh model of the capacitance [4] as

$$C_{gs} = C_{gs0} + C_{gs1}(1 + \tanh(P_{gs0} + P_{gs1}V_{gs} + P_{gs2}V_{gs}^2 + P_{gs3}V_{gs}^3))(1 + \tanh(P_{ds0} + P_{ds1}V_{ds} + P_{ds2}V_{ds}^2)) \quad (14)$$

We observe that this equation fails to converge for any further increase in the number of terms of the polynomial. The root mean squared error for the fitting is 22.49. The error in our model is approximately 10 times smaller than this function. However, we use a large number of parameters in our model when compared to the tanh model which is easier and often used.

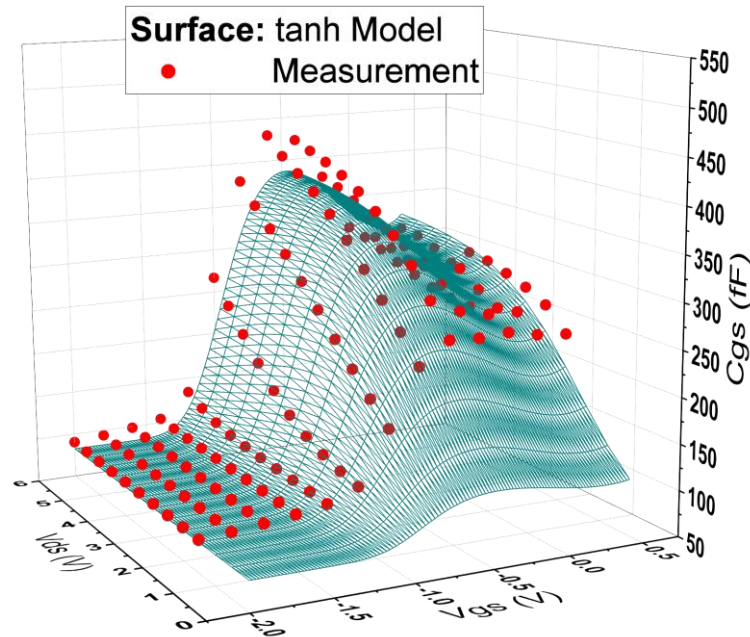


Fig. 5. The extracted values compared with the tanh model often used for modelling.

## V. Conclusion

Volterra analysis is a helpful tool for analyzing the distortion generated in an amplifier due to its insight into the generation mechanisms whilst offering a designer better choice to handle linearity. In this work, we propose a polynomial based model for  $C_{gs}$  and  $C_{gd}$  which enables to compute first, second, and higher components of the distortion originating from the non-linear intrinsic capacitances directly from simulation. Additionally, the proposed model is more accurate than the “tanh” function, often used to model  $C_{gs}$ .

## VI. Acknowledgements

The authors acknowledge Dr. Roberto Quaglia, University of Cardiff for the characterization of samples. This work is supported by funding from ESA.

## VII. References

- [1] J. P. Aikio and T. Rahkonen, “Detailed distortion analysis technique based on simulated large-signal voltage and current spectra,” *IEEE Trans. Microw. Theory Tech.*, vol. 53, no. 10, pp. 3057–3066, Oct. 2005.
- [2] J. P. Aikio and T. Rahkonen, “Reliability of polynomial  $I_{DS}/V_{GS}/V_{DS}$  model fitted using harmonic-balance simulation,” in *Proceedings of the 2005 European Conference on Circuit Theory and Design, 2005.*, vol. 3, pp. 89–92.
- [3] J. P. Aikio and T. Rahkonen, “A Comprehensive Analysis of AM–AM and AM–PM Conversion in an LDMOS RF Power Amplifier,” *IEEE Trans. Microw. Theory Tech.*, vol. 57, no. 2, pp. 262–270, Feb. 2009.
- [4] I. Angelov, N. Rorsman, J. Stenarson, M. Garcia, and H. Zirath, “An empirical table-based FET model,” *IEEE Trans. Microw. Theory Tech.*, vol. 47, no. 12, pp. 2350–2357, 1999.
- [5] S. Maas, *Nonlinear Microwave and RF Circuits*, Second Edi. Artech, 2003.

- [6] I. Angelov, "Empirical Nonlinear IV and Capacitance LS Models and Model Implementation," in *MOS-AK Baltimore*, 2009, p. 51.
- [7] J. Vuolevi and T. Rahkonen, *Distortion in RF Power Amplifiers*. Artech House, INC, 2003.
- [8] N. B. De Carvalho and J. C. Pedro, "A comprehensive explanation of distortion sideband asymmetries," *IEEE Trans. Microw. Theory Tech.*, vol. 50, no. 9, pp. 2090–2101, 2002.
- [9] K. A. Remley, D. F. Williams, D. M. M. P. Schreurs, and J. Wood, "Simplifying and interpreting two-tone measurements," *IEEE Trans. Microw. Theory Tech.*, vol. 52, no. 11, pp. 2576–2584, 2004.
- [10] N. Poluri, "Contributing to Second Harmonic Manipulated Continuum Mode Power Amplifiers and On-Chip Flux Concentrators," PhD Thesis, The University of Sheffield, 2020.
- [11] N. Poluri, M. M. Desouza, N. Venkatesan, and P. Fay, "Modelling Challenges for Enabling High Performance Amplifiers in 5G / 6G applications," in *28th international conference on Mixed Design of Integrated Circuits and Systems (MIXDES)*, 2021.